Title

The fully automated bat (FAB) flight room: A human-free environment for studying navigation in flying bats and its initial application to the retrosplenial cortex

Authors

Genzel, Daria
Yartsev, Michael M

Publication Date

2021

DOI

10.1016/j.jneumeth.2020.108970

Peer reviewed

HHS Public Access

Author manuscript

J Neurosci Methods. Author manuscript; available in PMC 2022 February 19.

Published in final edited form as:

J Neurosci Methods. 2021 January 15; 348: 108970. doi:10.1016/j.jneumeth.2020.108970.

The Fully Automated Bat (FAB) Flight Room: A Human-Free Environment for Studying Navigation in Flying Bats and its Initial Application to the Retrosplenial Cortex

Daria Genzel[1,2], **Michael M. Yartsev**[1,2,*]

[1]Helen Wills Neuroscience Institute, UC Berkeley, Berkeley, 94720, United States.

[2]Department of Bioengineering, UC Berkeley, Berkeley, 94720, United States.

Abstract

Background—Bats can offer important insight into the neural computations underlying complex forms of navigation. Up to now, this had been done with the confound of the human experimenter being present in the same environment the bat was navigating in.

New Method—We, therefore, developed a novel behavioral setup, the fully automated bat (FAB) flight room, to obtain a detailed and quantitative understanding of bat navigation flight behavior while studying its relevant neural circuits, but importantly without human intervention. As a demonstration of the FAB flight room utility we trained bats on a four-target, visually-guided, foraging task and recorded neural activity from the retrosplenial cortex (RSC).

Results—We find that bats can be efficiently trained and engaged in complex, multi-target, visuospatial behavior in the FAB flight room. Wireless neural recordings from the bat RSC during the task confirm the multiplexed characteristics of single RSC neurons encoding spatial positional information, target selection, reward obtainment and the intensity of visual cues used to guide navigation.

Comparison with Existing Methods—In contrast to the methods introduced in previous studies, we now can investigate spatial navigation in bats without potential experimental biases that can be easily introduced by active physical involvement and presence of experimenters in the room.

[*]To whom correspondence should be addressed. myartsev@berkeley.edu.

Author Contributions

D.G. and M.M.Y. designed the study, analyzed the data and wrote the manuscript. D.G. implemented the technical components of the flight room and conducted the experiments

Ethics statement

All experimental procedures were approved by the Institutional Animal Care and Use Committee of the University of California, Berkeley.

Conflict of interest

The authors declare no competing/financial interests.

Conclusions—Combined, we describe a novel experimental approach for studying spatial navigation in freely flying bats and provide support for the involvement of bat RSC in aerial visuospatial foraging behavior.

Keywords

Bat; 3D navigation; novel behavioral framework; Retrosplenial cortex

Introduction

Bats are emerging as a prominent mammalian model system for studies of spatial behavior, including navigation [1,2]. This endeavor is propelled by the development of methodologies for wirelessly recording neural activity during flight [3-5]. However, all neurophysiological studies in flying bats up until now have necessitated the direct and continuous involvement of human experimenters during both training and testing. This presents a major challenge since the necessity for physical involvement of human experimenters in studies of spatial behavior (i) introduce potential experimental biases and variability [6-8], (ii) reduce experimental throughput and reproducibility, (iii) prevent the animal from engaging in free self-paced navigation behavior [9,10] and (iv) limit the complexity of possible tasks that could be utilized to study neural circuits. To overcome these limitations, we developed a novel experimental framework – the fully automated bat (FAB; Fig 1) flight room. Here, a complex experimental environment can be programmed externally and applied to a sufficient number of animals in a reproducible manner. Importantly, in this controlled environment bats are free to engage in a self-paced, ethological foraging behavior without human intervention while enabling detailed quantification of their spatial behavior and underlying neural activity.

Here, we demonstrate the utility of the FAB flight room for studying a multi-target, cue-varying, visual-based navigation and underlying neural activity in Egyptian fruit bats, *Rousettus aegyptiacus*. While bats are renowned for their unique sense of echolocation [11,12], most bats also rely on other sensory modalities to negotiate their environment [13-15]. For instance, when navigating in large open spaces it is difficult for a bat to rely on echolocation alone, due to rapid atmospheric attenuation, especially in the ultrasonic range [12,16]. Indeed, all non-echolocating, and many of the echolocating bats use vision as a sensory input and can be guided by distal visual landmarks [17-19]. This is also assumed to be the case for the goal-directed navigation of Egyptian fruit bats in the wild [2,18]. We therefore trained bats of this species on a goal-directed navigation task where individuals had to approach in flight one of four randomly selected targets to obtain food reward. The correct target on each trial was marked by a visual cue, delivered via a small LED positioned at each target (Fig 1). Using the flight room's custom software, we could vary on each trial not only the rewarded target but also the intensity of the light cue guiding the bat's choices (Material and Methods). This in turn allowed us to obtain a detailed psychometric description of the bat's visuospatial foraging behavior.

In parallel, we synchronously recorded neural activity from a brain region that across species has been widely associated with visual-based navigation – the retrosplenial cortex

(RSC, Fig 2A-C, [20-24]), yet never studied before in bats, nor in other species during three-dimensional navigation. While neurophysiological studies in navigating bats focused primarily on the hippocampal formation (but see Kothari et al., 2018 [25]), research in other mammals has highlighted the importance of other, non-hippocampal, structures for spatial behaviors. In particular, the RSC - a cortical region outside the hippocampal formation - has been attributed a wide variety of roles in supporting navigation behavior, such as encoding information related to spatial memory, context, reward, imagination and future planning [26-33], especially when involving the visual domain. In rodents the RSC is densely innervated by inputs from visual areas [34], making it a prime candidate for facilitating visuospatial navigation. Yet, because this region has never been investigated in bats before, its potential contribution to the bat's foraging behavior remains entirely unknown. We therefore aimed to leverage the utility of the FAB flight room to obtain important insight into the bat's ability to forage based on visual cues and ask how visuospatial variables are encoded in the RSC.

We find that Egyptian fruit bats can be efficiently trained in the FAB flight room and develop highly reproducible and stable spatial behavior when engaged in multi-target, visuospatial navigation (Fig 2D). Neural recordings from the RSC of bats engaged in the task reveal a multiplexed representation of relevant task variables extending from the preparatory period before flight, spatial movement during flight and lastly, representation of reward obtainment after landing. These results extend the proposed role of RSC in aerial navigation and further suggest that much of the information that could be utilized by the bat for solving complex forms of spatial navigation may already be present upstream of the hippocampal formation.

Material and Methods

Animals

Neural activity was recorded from three adult male Egyptian fruit bats, *Rousettus aegyptiacus,* a megachiropteran, Old-World fruit bat. Four additional adult male bats were utilized for obtaining behavioral psychometric functions. All seven bats that participated in this study were removed from the breeding colony at UC Berkeley. As these bats were initially wild-caught, we could not precisely estimate their age. Based on physiological measures we estimate their age to be between three and 10 years old. During the measurements of the initial psychometric functions all bats were housed together in a large cage (81x48x94cm) in a humidity- and temperature-controlled room with a 12-hour reversed light-dark cycle. All experiments were conducted during the dark cycle. During the neural recordings an implanted bat was housed with a companion bat. The bats received a banana-melon-honey smoothie during training sessions 5-6 days a week and water *ad libitum*. A fruit-vegetable mix (consisting of apples, pears, melons, grapes, plums, kale, carrots and sweet potatoes) was given *ad libitum* on resting days (1-2 days a week).

Technical setup

To investigate cortical network computations in freely flying and behaving bats without human involvement, we developed a fully automated training and recording system, the

FAB flight room (Fig 1). In an acoustically, electrically and RF- shielded room (5.6x5.2x2.5 m) four landing platforms with associated cue units (Fig 1A) were positioned at one end of the room and a hanging perch was placed on the other end of the room (Fig 1B). Each platform had an IR-light barrier (Adafruit Accessories IR Break Beam Sensor - 5mm LEDs, Adafruit Industries, LLC, MA, USA) and motor (RB 35, Modelcraft, Modelcraft Co., Plymouth, CT, USA) for pushing an attached food filled syringe (Fig 1C). Cues were presented via custom-made cue units consisting of a white LED (round top 5 mm LED incl. 150Ω resistor, AMX3d Inc., Il, USA), loud speaker (Discovery Tweeter R2604/833000, Scanspeak, Videbæk, Denmark) connected to an amplifier (Servo 120A, Samson Technologies, NY, USA) and microphone (fairly flat frequency response up to 70 kHz, Earthworks M50, Earthworks Inc., NH, USA) which was connected to a preamplifier (OctaMic II, RME Synthax Inc., FL, USA) and recorded the echolocation calls (sampling rate 192 kHz). Two additional microphones (custom built from Knowles SPU0410LR5H-QB, IL, USA) also connected to the preamplifier were positioned in the middle of the long-axis of the flight room sides. All microphones were corrected to achieve flat frequency responses up to 96 kHz. Audio recordings were controlled with the Soundmexpro (HorTech gGmbH, Oldenburg, Germany) toolbox for Matlab (Matlab R2015b-R2019a, MathWorks, Natick, MA). The IR- light barriers and the motors were controlled through a stand-alone microcontroller system (Arduino Uno, Arduino, MA, USA) connected to the PC (Fig 1D). The bats' 3D position in space was tracked and recorded through Cortex (Cortex-64, Motion Analysis, CA, USA) retrieving the information from 16 high-speed video cameras (Raptor-12HS with 180 frames per sec, Motion Analysis, CA, USA) (Fig 1E). The tracking software monitored with millimeter-scale spatial resolution a necklace around the bats' neck consisting of five IR reflecting spheres (5 mm diameter). It is important to note that although the cameras of the tracking system generated a residue of red light, the behavioral response was not affected as it was entirely driven by the active LED at a target. Two additional USB cameras (Megapixel IP camera, ELP, Ailipu Technology Co. Ltd, Shenzhen, Guangdong, China) connected to Cortex allowed monitoring of the bats' activity from outside the room. A mesh bird netting (BirdBlock 64, Jobe's Easy Gardner Products, TX, USA) was stretched parallel to the ceiling below the cameras to limit the bats flying above the cameras' field of view, thereby reducing the accessible height to 2m. The combination of Soundmexpro (HörTech gGmbH, Oldenburg, Germany), a multi-channel professional soundcard system made up of an A/D-D/A converter (Ferrofish A16, Ferrofish GmbH, Germany) and an internal sound card (HDSPe MADI FX, RME Synthax Inc., FL, USA) allowed for perfect synchronization across all its input and output signals (Fig 1D). A wireless transceiver and logger system (radio link and Spikelog-16, Deuteron Technologies Ltd., Israel) recorded the neural activity continuously but was synchronized with the other in- and outputs via a trigger signal (Fig 1D). All signals were controlled and recorded through one PC running a fully-automated procedures written in-house in Matlab.

Synchronization

To ensure synchronization of all recording systems with the bat's behavior, a trigger signal from the stand-alone microcontroller system (Arduino) was sent to (1) the 3D flight recording system (Cortex), (2) acoustic recording system (Ferrofish & HDSPe MADI FX) and (3) the transceiver of the neural recording system (Deuteron) as soon as the bat

interrupted one of the four IR-light barriers on the platforms. A custom-made adapter circuit stabilized the trigger signal such that it could be input to a COM port channel of the PC which the 3D flight system monitored (Fig 1D). The trigger signal was generated by setting one of the microcontroller's outputs to high (+5 V) and resetting to low after the audio recordings had been saved and the bat rewarded in the case of a correct decision. The neural recording system associated the trigger events with the continuous recording file by detecting the rising slope of the trigger signal. Important to note, the trigger signal was not sent to the logger itself but to the transceiver that synchronizes to the logger on regular intervals (~ every five minutes). This allowed for any necessary time alignment correction in case of clock-drifts. Similarly, the flight recording system, monitoring the COM port, identified the rising slopes and automatically saved the 3D flight information for a predetermined time before the trigger event. The acoustic system saved the trigger signal along with the microphone recordings. Synchronizing in this manner enabled an easy alignment of all recordings for a specified time duration before the bat landed on a platform.

Sensory cues

The visual cue consisted of one LED which could be varied in intensity through pulse-width modulation. As LEDs are bimodal (on or off), this is accomplished by applying a pulse-width modulation where the pulse width for activating the LED is reduced. This resulted in a percentage of the LED being on or off, ranging from 95% (= highest intensity) to 0.01% (= lowest intensity). The luminance for 95, 50, 10, 5, 1, 0.5, 0.1, 0.05 and 0.01% were measured with a luminance measurement tool (Thorlabs Optical Power Meter PM130D, THORLABS Inc., NJ, USA) at a distance of 4.5 cm positioned facing toward the LED and resulted in values of 1000, 132, 82, 56, 17, 10, 5, 4.5 and 4,2μWatt/mm^2, respectively.

Behavioral procedure

Bats were trained to approach and land on one of four platforms in a four alternative forced choice (4AFC) paradigm. The correct landing platform was indicated by the light cue and was the only one, for a given trial, where a bat could receive a reward. Achieving this behavior involved prior training steps where bats learned (1) to initially identify a target platform as a reward location, (2) to repeatedly land on a platform to receive a reward, (3) to approach not only one but at least two different targets to receive a food reward (here the light cue was activated at all four targets simultaneously and a reward could be received at all four), (4) to approach all four targets for a reward (here the light cue was activated at only one rewardable target at a time, a reward could only be received at this target and this target remained the only rewarded target until the bat correctly landed on its platform) and (5) to reliably approach a correct target where the light cue was activated (here after a wrong choice a random sequence determined which target would be activated). All training steps were conducted with automatic training procedures; the experimenter simply chose at the beginning of the session at what training step a bat was on. This decision was based on the bat's prior performance. By removing the experimenter's presence in the room or his/hers direct input from outside the room (e.g. manual control of reward time points), any potential experimenter biases are removed and performance differences between days or animals are solely attributed to the animals themselves rather than the experimenter that is running the session.

All seven animals were successfully able to proceed through all training steps and ultimately choose the correct target in a 4AFC-paradigm in a reliable manner. As soon as a bat correctly chose landing platforms based on activated light cues (> three consecutive days above 43% = significance level when calculated over 30 trials) the intensity of the cue was decreased in a staircase manner. Example daily performances for high and low intensity trials are shown for three bats in Figure 3A-C. For each session, before the staircase adjustment was applied, a bat received a minimum of five training trials at the 95% (highest) light intensity. This was done in order to ensure that the bat was concentrating and attending to the task. The staircase intensity steps were 80, 60, 40, 40, 10, 8, 6, 4, 2, 1, 0.5, 0.1, 0.05, 0.04, 0.02 and 0.01%. The light intensity was gradually reduced until a bat reached chance level (25% percent correct trials calculated over the last 30 trials). As soon as a bat reached its approximate chance level only intensities where less than 30 trials had been collected were presented in a random sequence with 80% intensities interspersed to ensure the bat's motivation. A psychometric function was then generated by calculating the percent correct performance over the last 30 trials for each obtained intensity value (excluding the 95% intensity). Resulting data points were fitted with a non-linear curve fit function (modified Weibull distribution; Fig 2D). General behavioral values are given in Table 1.

During neural recordings fewer intensities were presented in a random order (not in a staircase procedure as before) and chosen based on the prior measured performance for each bat: 80% intensity was chosen for each bat as the highest and 0.01% as the lowest intensity and two additional intensities (one slightly above and one slightly below the bat's measured threshold). This resulted in trials being grouped into high (80% and more) and low (less than 80%) intensities. Again, for each session, before the random presentation procedure was initiated, a minimum of five training trials were acquired at 95% (highest) intensity, ensuring the bat was engaging with the task. This intensity was also presented throughout the session if the bat's performance or motivation was declining. The psychometric functions were then again generated by calculating the percent correct performance over the last 30 trials for each obtained intensity value and fitting this vector with a non-linear curve fit function (modified Weibull distribution; Fig 3D-F). General behavioral values during the implant sessions are given in Table 2 and overall trial numbers for each light intensity during pre- and post-implant sessions are given in Table 3&4. Daily performance for three implanted bats is shown in Figure 3G-I. For each trial flight and echolocation activity and the bat's decision was recorded by the visual and acoustic tracking systems. IR-light barriers at each of the landing platforms controlled the end of a trial, for correct trials the presentation of a food reward and the retrieval of all recordings. During the initial psychometric function measurements, the last seven seconds prior to light barrier interruption were recorded. During the neural recording sessions, the last ten seconds for Bat 3 & 7 and 15 seconds for Bat 1 were recorded.

Activation of the visual cue at a cue unit was determined by a combination of random sequences and the animal's performance history. During the neural recording sessions before a bat was released into the flight room and after it had performed the behavioral task, neural activity was recorded for an additional five to ten minutes while the bat remained in its transport cage. There, the bat could move around but not fly. These periods served as a baseline recording period independent of any task variables or flight activity. Overall, each

bat had a session time of 60 – 90 minutes for the exploration of the space during which the experimenter did not interfere. This allowed the bats to learn and gather experience about the spatial environment at their own pace without human influence and bias. This automated training procedure therefore allowed training without continuous supervision, resulting in a sufficient number of trained animals and providing time to prepare parallel procedures simultaneously. Applying this setup design and paradigm we were able to automatically present cues, control rewards, have information about the bats' decision at targets, record their echolocation activity (via six microphones), track their 3D spatial position (via 16 cameras) and wirelessly record neural activity during flight.

Task variables

Task variables were defined as followed: (i) cued target, (ii) approached target, (iii) light (cue) intensity and (iv) reward outcome. The target variables (cued and approach) consisted of four target conditions (Targets 1-4), the light intensity variable was defined as either low (intensities <80%) or high (intensities >=80%) and the reward outcome variable consisted of two conditions (obtained or not-obtained reward, corresponding to correct or incorrect decisions, respectively).

Flight trajectories

3D flight trajectories (seven, ten or 15 seconds prior to landing on a target platform) were reconstructed off-line by first transforming the recording files (.cap) into C3D files (with a custom-designed plugin for the Cortex software, Motion Analysis). These files were then processed by a custom-designed Matlab code and the resulting trajectories were smoothed in the following manner: any missing tracking points (e.g., due to momentary obstruction) and trajectory points which differed more than three mm to successive trajectory points were replaced with interpolated values using a custom-written linear interpolation function by W. O. Brimijoin, 2014 and smoothed by a Hanning window application (custom-written function by W. O. Brimijoin, 2014). Interpolation between two points was only done for a maximum of four trajectory points. Trajectories were then examined and corrected again by removing trajectory points which differed more than 15 mm to successive trajectory points and replaced (along with three trajectory points before and after) with interpolated values. All processes were conducted for all three spatial dimensions (X, Y and Z) of a trajectory. Example flight trajectories during one session are depicted in Figure 4 A-E.

To analyze the stereotypy of flight trajectories toward each target, we compared for each session all trials to each other in a pairwise manner. This was done by sliding a window of 500 msec with an overlap of 100 msec over the shortest trial time of the two trials and computing the 3D Euclidean distance. Trial comparisons were separated into trials toward the same target and trials toward different targets (Fig 4F). A linear mixed model tested for an effect of target choice and its interaction with the time before landing. To test the hypothesis that the light cue's intensity could affect the flight behavior of the bats (lower intensity could introduce decision insecurity during target approach and thereby slight deviations in the flight trajectories to a target), comparisons were made only between trials toward the same target (Fig 4G) but here trials were grouped whether both had a high light intensity (>=80%) or differed in their intensity (one trial with light intensity at or above

80% and the other with light intensity below 80%) or both had a low intensity (< 80%). A linear mixed model tested for an effect of intensity and its interaction between the time before landing (fitlme function in Matlab).

Behavioral periods

Three different stages were defined during the task: the preparatory period (three seconds before flight), flight and reward period (three second period after the bat interrupted the IR beam on the landing platform). This separation is based on the outcome of prior studies from other species revealing the RSC's involvement in representing relevant sensory cues during visual-based spatial behavior [20-22] as well as the reward outcome [31]. We therefore aimed to investigate the neural activity during the flight preparation, the flight itself and during reward obtainment. The reasoning behind the preparatory period was due to the initial performance measurements (before implant) which revealed that all bats very directly approached each target indicating that they were making a choice already at the perch short before take-off. The preparatory and flight stages were extracted by calculating the first derivative of the trial's flight trajectory, i.e., velocity. Flight time was determined as velocity values above 0.1 mm/msec and preparatory periods as the three seconds before the velocity reached this threshold. The start of reward period was triggered by the beam break.

Echolocation analysis

The Egyptian fruit bat echolocation signal is produced through tongue clicking, resulting in a double click separated by ~10-30 msec in the frequency range of ~10-90 kHz and intervals of one double click to another of ~100 msec [35,36]. Seven, ten or 15 seconds of echolocation activity prior to landing on a target platform were recorded via six microphones (one at each target location and one on each side of the middle of the longer flight axis). A custom-designed Matlab based code was applied for extracting echolocation information. Each of the six recording channels was band-pass filtered (10 - 40 kHz) with an 8^{th} order Butterworth and then analyzed for peaks (findpeaks function in Matlab, threshold set to 0.005 V). Example filtered echolocation recordings for each of the six microphones are shown in Figure 4H. Peak differences less than ten msec were removed by comparing the voltages of the peak indices and deleting all but the maximum. As a result, the time point for each of the double clicks of the echolocation signal was extracted. For each time point during a trial both the bat's and each microphone's spatial position is known (in X-, Y- and Z-dimensions) and the distance of the bat to each microphone can be calculated. As the flight position was tracked with a frame rate of 180 frames per second, but sound was recorded with a sampling rate of 192000 samples per second, each channel was checked for echolocation clicks occurring up to the time point corresponding to a video frame and occurring after the time point of the previous video frame (but corrected for sound travel time of 340 meter per second). This allowed extraction of the bat's spatial position for each echolocation click.

Surgical procedure

Anesthesia and surgical procedures generally followed those described previously in detail for Egyptian fruit bats [37]. Surgeries were performed to implant a 4-tetrode microdrive on each bat. Anesthesia was induced using an injectable cocktail of ketamine (22 mg/kgBW),

dexamedetomidine (0.09 mg/kgBW) and midazolam (0.31 mg/kgBW). Subsequently, the bat was placed in a stereotaxic apparatus (Model 942, Kopf, CA, USA) and anesthesia was maintained throughout surgery by repeated injections (roughly once per hour) of an anesthesia maintenance cocktail of dexamedetomidine (0.125 mg/kgBW), midazolam (2.5 mg/kgBW) and fentanyl (0.025 mg/kgBW). Depth of anesthesia was continuously monitored by testing toe pinch reflexes and measurement of the bat's breathing rate. The bat's body temperature was measured using a rectal temperature probe (FHC, ME, USA) and kept constant at approximately 35-36°C using a regulated heating pad.

Each bat was implanted with a four-tetrode lightweight microdrive (Harlan 4 Drive, Neuralynx; weight 2.1 g). Tetrodes (~45 μm diameter) were constructed from four strands of platinum-iridium wire (17.8 μm diameter, HML-insulated), bound together by twisting and then melting their insulations. Tetrode applications in the RSC for recording neural activity have been successfully demonstrated in previous studies in rodents [24,31,32,38]. Each of the four tetrodes was loaded and glued separately into a telescoped assembly of polyimide tubes mounted into the microdrive. The tetrodes exited the microdrive through a guide cannula in an approximately rectangular arrangement with 300-600 μm horizontal spacing between tetrodes. Each tetrode could be moved independently via a separate drive screw. On the day before surgery, the tip of each tetrode was cut flat using high-quality scissors (tungsten-carbide scissors with ceramic coating; FST, CeramaCut, FST, CA, USA) and gold-plated (Neuralynx, MT, USA) to reduce the impedance of individual wires to 0.4-0.6 MΩ (at 1 kHz).

While the bat was under anesthesia, the skull was micro-scarred to improve subsequent adhesion, and a circular opening (craniotomy of 1.8 mm diameter) was made in the skull over the right hemisphere with the electrode positioning adapted to established procedures and existing brain atlases (Eylam et al., unpublished brain atlas for the Egyptian fruit bat; M. Witter, personal communication). The targeted stereotaxic coordinates for the RSC implant were at 1.7 mm from midline and 4.7 mm anterior from the sinus. The RSC extends from −1.5-4 mm in depth from surface level when approached at a 20° off the vertical axis. After removal of the dura, the microdrive was lowered with the tip of the microdrive's guide tube placed on the brain surface. The craniotomy was then filled with a biocompatible elastomer (Kwik-Sil™, World Precision Instruments, FL, USA) to protect the brain. A bone screw (19010-00, FST, CA, USA) with a soldered stainless-steel wire (.008" coated, A-M Systems, WA, USA) was fixed to the skull in the frontal plate, and served as a ground screw after its electrical connection to the dura was verified. An additional set of three to five bone screws were fixed to the skull and served as anchor screws for the mechanical stability of the implant. The bases of the screws were then covered with a thin layer of quick adhesive cement (C&B Metabond®, Parkell, NY, USA) which held the screws firmly to the skull; dental acrylic was then added to secure the entire microdrive to the screws and to the skull. At the end of the surgery, bats were given the analgesic meloxicam (Metacam®, Boehringer Ingelheim, Germany) and, if needed, the anti-inflammatory drug dexamethasone. The bat was treated with antibiotics for one week and with pain medication for three days, post-op.

Neural Recordings

After the bat had recovered from the surgery it was returned to behavioral training as described before and neural activity from all tetrodes was recorded using a wireless neural data logging system (Neurolog-16, Deuteron Technologies Ltd., Israel), which amplifies the voltage signals from the 16 channels of the four tetrodes, performs analog-to-digital conversion at a sampling rate of 29.29 kHz, and stores the digitized data on an on-board SD card, mounted together with the battery on the top of the microdrive. The neural signals (for example trace see Fig 2C) were synchronized through the radio link transceiver with the PC running the behavioral software. The system has a bandwidth of 1 Hz - 7 kHz, records voltage with a fine resolution of 3.3 mV and has a low level of noise generally close to the limit of Johnson noise from the impedance of a given source. This recording system is light-weight (9.9 g, including battery and plastic casing). The Egyptian fruit bats used in our experiment weighed more than 150 g and carried the recording system with ease, as expected from previous experiments using wireless recording systems with heavier or comparable weights during free flight for over an hour and covering multiple kilometers [3,4].

After a recording session was concluded for the day, we connected the tetrodes to a wired recording system (Digital Lynx, Neuralynx, MT, USA) to monitor the neural signals and advance the tetrodes. Tetrodes were moved downward once every one to two days (in a range of 100 ±165 μm), in order to record single units and local spiking activity at new sites. All recordings were then retrieved off-line after disconnecting the head-stage from the bat.

Preprocessing of neural data

Neural responses were analyzed off-line by running the raw traces through a custom-designed Matlab script. Spikes were detected by band-pass filtering the raw voltage traces using a 6th-order Butterworth filter with cut-off frequencies of 600 and 6000 Hz. For each recording channel and each session, a voltage threshold was set as the following quantity: the difference between the 75^{th} percentile and the median of the voltage trace, divided by the 75^{th} percentile of the standard normal distribution, and multiplied by a factor of three [39]. Each time the voltage on one recording channel crossed its threshold, the peak voltage was detected and seven samples before and 24 samples after the peak were extracted, resulting in a vector of 32 samples (1.09 msec) from each channel of the tetrode. These extracted vectors were then used for single spike analysis in the cluster sorting software (SpikeSort 3D, Neuralynx, MT, USA) through which 438 single-units were identified. As shown in previous applications [3] wing beats and other artifacts were easily distinguishable from neural spikes in both the raw recording traces as well as during the clustering process, ensuring that spike detection was not contaminated. Both the trigger signals for synchronization of the systems and the IR tracking system also did not interfere with the neural recordings.

Calculation of spike rates

Following the spike sorting, further analysis was done via custom-made Matlab scripts. Only single-units which had at least one spike on 60% of the trials were included for further analysis. This resulted in 179 valid single units (41% of all identified units).

The spiking events of each unit were sorted according to the trial type in which they had occurred. The spike times for each trial were then divided into preparatory period, flight period and reward period, extracted by calculating the first derivative of the trial's flight trajectory (see velocity analysis). Note, that a trial could be shorter than the recorded ten or 15 seconds if trial times overlapped. The spike times during the flight period were translated into position in space, the preparatory period was defined as three seconds before flight and the reward period was defined as three seconds after the bat had landed at a target. Preparatory periods less than three seconds were excluded from analysis. All valid flight, preparatory and reward periods for different task variables (target, intensity and reward, respectively) were then collected, to calculate the mean spike rate over all trials for a task variable. During flight this was done by dividing the sum of spike events along a spatial axis (bin width of 100 cm) by the sum of the time spent in those bins and processing the extracted rate with a gaussian smoothing window (10 samples = 17% of the vector length). To ensure the analysis of flights only towards the targets, the last three seconds (based on mean flight durations for all bats, see Table 1&2) before landing were included. Similarly, spike rates during the preparatory and reward period were calculated by dividing the sum of the spike events along a temporal axis (bin width of 100 msec) by the number of trials and processing the extracted rate with a gaussian smoothing window (5 samples = 17% of the vector length). In general, spike rates were only included for analysis for a task variable if at least 5 trials per task variable condition were presented during a session (e.g. four targets or the two light intensities - low/high). If a neuron was analyzed for multiple task variables at least 5 trial per each task variable condition had to have occurred during a session (this was valid for 118 units).

To evaluate encoding strength for the intensity and reward task variables during the preparatory and reward periods, mean spike rates for one task variable condition were compared in a one-way ANOVA-test (anova1, Matlab) with the mean spike rates for the other task variable condition. This comparison was termed as significant for p values < 0.05. To evaluate encoding strength for task variables during flight, mean spike rates for one task variable condition were compared in a two-way ANOVA-test (anova2, multiple comparison corrected, Matlab) with the mean spike rates for the other task variable conditions. This analysis tested for the effect of the task variable condition, the spatial position along the trajectory and the interaction of task variable condition with position. This comparison was termed as significant for p values < 0.05.

Demixed principal component analysis

For the demixed principal component analysis (dPCA) [40] for each unit mean spike rates for different task variables combinations were extracted as detailed in *Calculation of spike rate*. Here however, for each trial, spike events were represented in time for all periods (preparatory, flight and reward) and each period was time-warped to the same length of 150 samples. The resulting spike rate was then processed with a gaussian smoothing window (150 samples = 33% of the vector length). Results of the analysis did not differ when using smaller gaussian windows (e.g. 80 samples). This resulted in 16 combinations (four target x two intensity x two reward conditions). The missing task variables for each unit were filled with a steady mean spike rate calculated over the spike rate of all task variable combinations.

dPCA analysis was performed applying Matlab codes (dpca, dpca_explainedVariance and a modified version of dpca_plot; free code available online from Kobak et al., 2016, component number set to 30).

Histology

Histology was done as previously described [37]. Each bat was given a lethal overdose of sodium pentobarbital and, with tetrodes left *in situ*, was perfused transcardially using a flush of 200 ml phosphate-buffered saline followed by 200 ml of fixative (3.7% Formaldehyde in phosphate buffered saline). The brains were then removed and stored in fixative. Subsequently, a cryostat was used to cut 40 μm coronal sections of the brains. The sections were Nissl-stained with cresyl violet, and cover-slipped. Digital images were taken of each section using an Axio Scan system (Zeiss, NY, USA). These images were used to identify the recording locations (Fig 2A, B). RSC locations were verified via existing brain atlases for this bat species (Eylam et al., unpublished and M. Witter, personal communication).

Results

Experimental setup and training in the FAB flight room

Seven bats were successfully trained to choose the correct target in a four-alternative forced-choice (4AFC)-paradigm. All animals rapidly progressed through training steps of identifying and then approaching one, two and ultimately four platforms to receive a food reward and finally associating a light cue with a correct target (Material and Methods). A fully trained animal flew in darkness from the perch to one of four targets (the correct target marked by an activated small LED serving as the light cue, Fig 1A) in a goal-directed manner (Fig 1B). The bat then landed on the target's platform and in doing so, disrupted an IR-light barrier (Fig 1C) monitored by the behavioral system (Fig 1D). Disrupting the IR-light barrier automatically ended the trial and, if the bat's choice was correct, triggered a reward by activating a feeder motor positioned under the platform (Fig 1C). Furthermore, the trigger signal was simultaneously sent to (i) the audio recording system (see Material and Methods), (ii) the three-dimensional (3D) monitoring, video system (Motion Analysis) and (iii) the neural recording software (Deuteron) – thereby allowing precise synchronization of all system components (Fig 1D, see Material and Methods). The 3D positional information, as well as the bat's echolocation times that occurred before the trigger were saved for each trial along with additional relevant task information (trial number, target identity, light intensity, target choice and trial duration). All acoustic events in the room were recorded by six ultrasonic microphones (two mounted on the room's side walls and four at the targets). The 3D position of the bat was determined in real-time by an array of 16, ceiling-mounted, high-speed video cameras (Fig 1E) which tracked a necklace (made of IR-light reflecting beads) on the bat's neck. The neural recordings were continuous but synchronized to each trigger event of each trial. As soon as all IR-light barriers had been uninterrupted for a minimum of three seconds, a new trial was initiated by activating the light cue at a target. This step insured that the bats had to leave the targets before a new trial was initiated.

After the initial phase of training in which bats learned to reliably approach the target with an activated light cue at their own volition, the light intensity was gradually reduced in a staircase manner and psychometric functions were measured for all bats (see Material and Methods). The small diameter LED (Material and Methods) was inactivated between trials. The number of psychometric function measurement sessions, trial times, number of trials and psychometric thresholds for all seven bats are detailed in Table 1. The resulting psychometric functions for all bats are shown in Fig 2D. The main reason for measuring light intensity thresholds was to obtain a quantitative understanding of the bats' performance as a function of light-cue intensity. The overall performance remained reliably above significance level for the high intensity trials during the entire period of measuring the psychometric function (example curves for three bats are shown in Fig 3A-C). After completing these initial measurements and training, all seven bats were released back into their home colony and recaptured as needed, thereby testing whether longer time breaks between training and implant resulted in performance degradation. By training multiple animals initially, we can compare performance among many individuals (including weight, gender and age differences) and choose (dependent on the research question) which individual to record from. As the purpose of this study was to demonstrate the FAB room's functionality, we choose individuals which throughout the sessions were constant in their performances. These three bats (numbered as 1, 3 and 7 in Table 1) were recaptured after several months (16, three and six months, respectively) and chronically implanted with a tetrode-based microdrive (see Material and Methods) and their psychometric functions re-measured for a select number of light intensities (based on their initial threshold measurements; see Material and Methods, Table 2 & Fig 3D-F). We found that the overall performance remained again reliably above significance level for high intensity trials (Fig 3G-I), demonstrating that it was possible to pretrain animals and implant and record even up to 16 months later without performance degradation. It is important to note that not only was the relatively high performance maintained but this level was achieved very rapidly and independently of the time between initial training and testing (Fig 3G-I). This suggests training in the FAB flight room resulted in robust learning that was retained for extended periods of time (months or years) and that the implant had no negative effect on the bat's behavior or performance. Combined, these results underscore the utility of the FAB flight room for efficiently training multiple bats in parallel with high and reliable performance outputs while facilitating free exploration without human interference.

Flight behavior in the FAB flight room

For studying goal-directed spatial navigation in the laboratory it is important to obtain reproducible spatial behavior that allows for trial-based analysis. We hence evaluated the bats' spatial behavior in the room by analyzing their 3D flight trajectories. The bat's 3D position was carefully monitored using a large array of 16 high-speed video cameras and the flight trajectories were reconstructed off-line (Material and Methods). We assessed the variability of the flights with respect to the different task variables, such as the rewarded target, light intensity and choice behavior. Fig 4A-E shows all trials recorded for one bat during a typical example session. Panels A and B show the 3D flight trajectories for trials separated into correct (A) and incorrect (B) trials and color-coded by light intensity (see color bars). Fig 4C-E presents the same flight trajectories but now also shown as a function

of time and separated by the three canonical dimensions (X, Y and Z). Trials are again color-coded for correct and incorrect trials (green and magenta, respectively). The bats' flight behavior was highly stereotyped and target-oriented, which is also reflected in short flight times for each bat (Table 1&2). The reproducibility of the flight behavior persisted irrespective of the bats' target of choice. In detail, flights to the same target were very similar to each other as compared to flights to different targets (Fig 4F), irrespective of cue intensity (Fig 4G). This underscores the reliable and reproducible flight behavior exhibited by the bats under these conditions.

Combined, these behavioral results demonstrate that bats robustly engaged in the visuospatial foraging task and exhibited highly reproducible flight patterns in 3D space that were independent of task variables. It is important to note that during the experiment the bats were not restricted in how and when they approached the targets and therefore the length and stereotypy of the flight paths was not enforced. Nevertheless, these short approaches to the targets are reminiscent of the highly stereotyped, albeit longer, flight patterns this species is known to exhibit during navigation in the wild [2,18]. Importantly, the robust behavior exhibited by the bats in the FAB flight room allows for a quantitative analysis of trajectories through 3D space during a self-paced, exploratory task, an important factor for the evaluation of simultaneously recorded neural activity.

RSC neural activity

The FAB room's functionality allowed us to simultaneously record neural activity wirelessly from the RSC (Fig 2A-C) of three bats as they performed the visuospatial foraging task. For analysis of spike rates, we defined three distinct behavioral periods corresponding to the: (i) preparatory period (before flight), (ii) flight period and (iii) reward period (after landing) (Material and Methods). Fig 5A-I show different temporal (Fig 5A-C) and spatial (Fig 5D-I) firing patterns of three example neurons. Fig 5A-C show all spiking events (black dots) for each neuron for the four different approached targets (colored background) during the different behavioral periods. Fig 5D-I shows all spiking events occurring during flight (red dots) overlaid on flight trajectories (gray lines) for trials ending at (Fig 5D-F) or cued by (Fig 5G-I) different targets. The first example unit (Fig 5A, D and G) activates during all three periods but in a spatially and temporally-selective manner. For example, note that while this unit generally activates at the beginning of flights to the different targets, spiking near the end of each flight occurs primarily when the bat approaches Targets #2 or #3, independent of whether they were cued or not. The second example unit (Fig 5B, E and H) is relatively silent during the preparatory period yet activates robustly at the beginning of flights to all targets, but not prior to landing. The third example unit (Fig 5C, F and I) fires robustly at the end of most flights, as well as during the reward period at Targets #2-4 but much less so at the beginning of flights, as was the case for Examples 1 and 2. These examples illustrate the mixed-selectivity of RSC neurons and we next systematically determined how, across the population, RSC single units' activity was modulated during the visuospatial foraging task.

We began by examining the neural activity during flight as a function of the bats' spatial position relative to either the approached or cued target. Due to the high stereotypy of

the flight paths starting at one end of the flight room and ending at the other, it was possible to describe the flight trajectory along a single spatial dimension extending from the perch to the targets. Mean spike rates were calculated for all trials where a given target was either approached by the bat or cued by the behavioral software. This allowed us to distinguish spatial target selection from cue presentation. Additionally, having privilege to the psychometric performance curve of each bat, we could also compare the neural responses between more difficult trials (leading to poorer performance; low light intensity trials) and easier trials (leading to better performance, high light intensity trials) (Material and Methods). Lastly, we also distinguished between correct (or rewarded) and incorrect (or unrewarded) decisions made by the bats. Differences in firing rates associated with the task variable (cued target, approached target, intensity or reward), the bat's position along the trajectory as well as the interaction of the position with the task variables were analyzed using a two-way ANOVA ($p<0.05$). Doing so revealed that the firing rates of 72.8% and 75.3% of the units (N=162) significantly differed based on which target was approached or cued, respectively (Fig 5J). It is important to note, that a unit's sensitivity for a target is not necessarily the same as a typical 'place cell' unit. Here, a unit sensitive for a given target can fire on different trajectories towards the target or when the target is cued by the light. A place cell would supposedly fire at specific spatial positions in the room (but see Wood et al., 2000[41]). Additionally, firing rates of 51.6% of the recorded units (N=126) significantly differed between low and high cue intensity trials and the firing rates of 48.3% of the units (N=178) fired differently for correct and incorrect trials (Fig 5J). Furthermore, approximately 92% of the units (see Table 5 for details of distributions) were spatially selective, activating at different rates along the trajectory (divided into three equal portions). Lastly, approximately 65% of the recorded RSC units exhibited a significant interaction between spatial position along the stereotyped trajectories and task variables (task variable x position interaction; see Table 5). Combined, these results suggest the RSC neurons can encode for the bat's spatial position and the different task variables (cued target, approached target, intensity and decision).

Having assessed the activity of RSC neurons during flight, we next turned to assess their activity when the bat was not flying, namely during the (i) preparatory period where the visual cue was present and (ii) during the reward period occurring after landing at the target. We found that during the preparatory period (before the bats took flight) nearly two thirds of the RSC neurons (62.9%, N=124, one-way ANOVA, $p<0.05$, Fig 5J) significantly changed their firing rates between low and high light intensity trials. When examining the neural modulation during the reward period, we found that 64.8% of the units were significantly affected by reward outcome, activating in different rates if the bat received reward or not after landing at the target (N=176, one-way ANOVA, $p<0.05$, Fig 5J). These results are in line with reports from other species highlighting the involvement of RSC in the representation of relevant sensory cues during visual-based spatial behavior [20-22] as well as in the representation of reward outcome [31]. Importantly however, the multi-variant structure of the task allowed us to go one step further and assess the selectivity of individual RSC neurons for multiple task variables simultaneously (or lack thereof). Doing so revealed that many of the RSC neurons were sensitive to multiple task variables. In detail, 44.1% of the units were jointly modulated by Target and Intensity, 47.5% were Target and Reward

modulated, 40.7% were Intensity and Reward modulated. Lastly, over a quarter of the recorded neurons (28.8%) were significantly modulated by all three task variables (N=118; Fig 5K). Comparing the units' selectivity for the approached targets resulted in the same distributions.

Lastly, and to further test in an unbiased manner whether single unit activity in the RSC was modulated by task relevant variables in a multiplexed fashion, we used the demixed principal component analysis (dPCA), as described in Kobak et al. (2016) [40]. dPCA decomposes neural population activity into few components and thereby captures data variance and exposes dependence on task variables. dPCA component labels were termed as the task variables namely, Target (T), Intensity (I), Reward (R) and the interaction of these. An additional component was defined as Condition independent (CI) which captures temporal modulations of the neural activity throughout the trial, irrespective of the task variables (for more details regarding CI components see Kobak et al. (2016) [40]). The percentages of variance explained by the different components, as identified by the dPCA, are shown in Fig 5L. We found that more than 50% of the neural variance was associated with the different task variables and their interactions. These results further validate that in freely flying bats engaged in a visuospatial foraging task, a large fraction of RSC neural variability can be attributed to the task variables and importantly, their interactions. It is important to note that application of dPCA to neural data in previous studies resulted in 65-90% of neural variance attributed to the CI components [40]. The relatively low proportion of variance (45%) attributed to the CI components in our data indicates that an even higher percentage of the neural variance can be accounted for by the task variables as compared to previous applications. Combined, these results suggest that not only do many neurons in the RSC modulate their firing rate in relation to individual task variables, but that in fact, most neurons are sensitive to multiple task-relevant variables in a conjunctive manner.

Discussion

The central goal of this study was to develop a novel experimental framework – the FAB flight room - that would allow investigating neural activity in freely flying bats while minimizing the necessity and involvement of human experimenters during training and testing. Up to now most studies concerning neural activity in bats have been done with anaesthetized [42-45] or constrained animals [46,47] making decisive conclusions of how different aspects of their behavior are encoded in the brain difficult. Only recently, has the development of more sophisticated tools allowed the study of neural circuits during free behavior [37,48-50] and flight [3-5,25,51]. But even with these new neurophysiological measurement tools at hand all bat studies necessitated the direct involvement and presence of humans throughout the experiment. In contrast to these prior studies, the novel experimental framework introduced here, allows bats to navigate freely in the experimental space and learn complex behavioral tasks at their own pace. We found that bats robustly engage with this setup and can be efficiently trained, resulting in robust training that persisted for months and even years. In detail, we found that (i) animals were reliably motivated for each session as reflected in sufficient trial numbers per session, (ii) progressed rapidly through training stages to ultimately perform the learned task at high performance levels, (iii) retained learned behavior for long periods of time after training, (iv) showed

stable performance levels and (v) exhibited highly reproducible and goal-directed flight paths. Furthermore, we argue that potential experimental biases that can be easily introduced by active physical involvement and presence of experimenters in the room are mitigated using this approach [52-55].

While the present study focused on visuospatial navigation behavior, this novel experimental setup provides flexibility concerning task type, complexity and spatial layouts of setup elements. Additionally, it allows testing different aspects of both neural and behavioral aspects in navigating bats. For example, utilizing the detectability of the bats' echolocation activity through the room's microphones we found that bats continue to echolocate throughout the task independent of which sensory mode the cue is presented. Although this insight is not novel, other studies (regarding microbat species) have shown that in bats echolocation and vision often complement each other [56-59], we now know that with this tool we can trigger visual or acoustic cue presentation in dependence of the animal's own request for information (done through echolocation). We thereby have a direct read-out of when an animal is acquiring and subsequently receiving information for navigation, allowing us to precisely measure the information uptake and integration. This can be taken further by timing manipulations to the bat's active acquisition of cue information thereby enabling assessment of neural dynamics and their influence on ongoing sensory motor integration during aerial navigation behavior. Additionally, the room's 3D tracking and neural systems allow for more than one bat to trained and recorded from simultaneously. This can be utilized to investigate the bats' intraspecific interactions as done in previous studies [37,51]. Further adaptions to the FAB room's application include i) easy extension of the number of targets, ii) repositioning each target's position and iii) manipulation of the spatial relationship between target platform (where the animals receive the reward) and its cue unit. Indeed, preliminary testing show that the cue units can be moved up to 86 cm along the X-Axis away from the target platform while keeping the animals' performance stable. This setup would allow disentangling the neural responses to the cue vs. the associated reward. The FAB room's initial application, as demonstrated here, is optimized for the flying bat, but by repositioning targets to the floor the FAB room can easily be expanded in its application to other species that are more common in laboratory settings, e.g. rodents.

As a proof of concept demonstration, we show that this setup can be seamlessly integrated with the wireless methodologies previously developed for recording neural activity in freely flying bats [3,4]. As a first application of this integrative approach, we examined how the RSC, a brain region never studied before in bats, is involved in multi-target, visuospatial foraging behavior. We found that the RSC not only encoded for the bat's position, cues used for navigation and the obtainment of reward, but that single RSC neurons were modulated in a multiplexed manner by multiple task variables. These findings complement previous studies in freely flying bats that have been nearly exclusively focused on the hippocampal formation [3,5,50,51,60-64].

These results are in-line with the proposed role of RSC in complex spatial behaviors that could complement computations occurring downstream in the hippocampus [23,65,66]. For example, lesions in the RSC are associated with remapping of hippocampal place cells in familiar environments [67], potentially due to subjects failing to identify the context,

thereby forcing the hippocampus to generate a new contextual representation [68]. It is conceivable, that by combining highly spatially-specific hippocampal responses with the multiplexed representation we found in the RSC, downstream brain regions could extract spatial representations at varying levels of selectivity, e.g. specific information about a particular event or general information of event occurrence [31]. The loss of such behaviorally-relevant, navigational information provided by the RSC might explain navigational impairments seen in subjects with RSC damage [31]. In humans, such difficulties in navigation abilities are termed topographical disorientation [69-71], and patients with RSC lesions report an inability to use familiar visual landmarks to navigate, despite retaining knowledge of the landmarks themselves [72,73]. Our findings in foraging bats support the notion that RSC could be important for mediating relationships among multiple pieces of spatial information that are necessary for successful navigational.

With this new experimental tool at hand, we can now gradually expand the concept of how spatial information, spatial variance and landmark reliability is computed by multiple cortical areas as well as by the hippocampal formation. The application of the FAB flight room goes far beyond this though, allowing the investigation of a variety of questions concerning the underlying neural computations during spatial behavior in freely foraging bats as these engage in free and unbiased spatial behavior.

Acknowledgements

We thank Yartsev lab members for discussions and thoughts on the project, N. Dotson and W. Zhang for comments on the paper, C. Ferrecchia and G. Lawson for veterinary oversight, OLAC staff for support with animal husbandry and care and M. Witter for anatomical guidance and histological verification of tetrode locations in RSC.

Funding/Support

This research was supported by NIH (DP2-DC016163), the New York Stem Cell Foundation (NYSCF-R-NI40), the Alfred P. Sloan Foundation (FG-2017-9646), the Brain Research Foundation (BRFSG-2017-09), the Packard Fellowship (2017-66825), AFOSR, the Kindship Foundation and the Searle Scholars Program (SSP-2016-1412) to M.M.Y; and a DFG (GE 2851/1-1) grant to D.G.

Data availability

All data from this study will be made fully available without restrictions upon request.

References

1. Genzel D, Yovel Y, Yartsev MM. Neuroethology of bat navigation. Curr Biol. 2018;28: R997–R1004. doi: 10.1016/J.CUB.2018.04.056 [PubMed: 30205079]
2. Geva-Sagiv M, Las L, Yovel Y, Ulanovsky N. Spatial cognition in bats and rats: from sensory acquisition to multiscale maps and navigation. Nat Rev Neurosci. 2015; 16: 94–108. doi:10.1038/nrn3888 [PubMed: 25601780]
3. Yartsev MM, Ulanovsky N. Representation of Three-Dimensional Space in the Hippocampus of Flying Bats. Science (80-). 2013;340: 367–372. doi:10.1126/science.1235338
4. Finkelstein A, Derdikman D, Rubin A, Foerster JN, Las L, Ulanovsky N. Three-dimensional head-direction coding in the bat brain. Nature. 2015;517: 159–U65. doi:10.1038/nature14031 [PubMed: 25470055]
5. Wohlgemuth MJ, Yu C, Moss CF. 3D hippocampal place field dynamics in free-flying echolocating bats. Front Cell Neurosci. 2018. doi:10.3389/fncel.2018.00270

6. Penley SC, Gaudet CM, Threlkeld SW. Use of an eight-arm radial water maze to assess working and reference memory following neonatal brain injury. J Vis Exp. 2013. doi:10.3791/50940
7. Van Driel KS, Talling JC. Familiarity increases consistency in animal tests. Behav Brain Res. 2005. doi:10.1016/j.bbr.2004.11.005
8. Mumby DG, Kornecook TJ, Wood ER, Pinel JPJ. The role of experimenter-odor cues in the performance of object-memory tasks by rats. Anim Learn Behav. 1995. doi:10.3758/BF03198944
9. Gallup GG, Suarez SD. An ethological analysis of open-field behaviour in chickens. Anim Behav. 1980. doi:10.1016/S0003-3472(80)80045-5
10. Suarez SD, Gallup GG. Open-field behavior in chickens: The experimenter is a predator. J Comp Physiol Psychol. 1982. doi:10.1037/h0077886
11. Neuweiler G. The Biology of Bats. New York: Oxford University Press; 2000.
12. Denzinger A, Schnitzler HU. Bat guilds, a concept to classify the highly diverse foraging and echolocation behaviors of microchiropteran bats. Front Physiol. 2013. doi:10.3389/fphys.2013.00164
13. Laska M. Olfactory discrimination ability in short-tailed fruit bat, carollia perspicillata (Chiroptera: Phyllostomatidae). J Chem Ecol. 1990;16: 3291–3299. doi:10.1007/BF00982099 [PubMed: 24263430]
14. Orbach DN, Fenton B. Vision impairs the abilities of bats to avoid colliding with stationary obstacles. PLoS One. 2010;5. doi:10.1371/journal.pone.0013912
15. Gonzalez-Terrazas TP, Martel C, Milet-Pinheiro P, Ayasse M, Kalko EKV, Tschapka M. Finding flowers in the dark: Nectar-feeding bats integrate olfaction and echolocation while foraging for nectar. R Soc Open Sci. 2016;3. doi:10.1098/rsos.160199
16. Schnitzler HU, Moss CF, Denzinger A. From spatial orientation to food acquisition in echolocating bats. Trends Ecol Evol. 2003;18: 386–394. doi:10.1016/s0169-5347(03)00185-x
17. Boonman A, Bar-On Y, Cvikel N, Yovel Y. It's not black or white-on the range of vision and echolocation in echolocating bats. Front Physiol. 2013;4. doi:10.3389/fphys.2013.00248
18. Tsoar A, Nathan R, Bartan Y, Vyssotski A, DellOmo G, Ulanovsky N. Large-scale navigational map in a mammal. Proc Natl Acad Sci U S A. 2011;108: E718–E724. doi:10.1073/pnas.1107365108 [PubMed: 21844350]
19. Wang D, Oakley T, Mower J, Shimmin LC, Yim S, Honeycutt RL, et al. Molecular Evolution of Bat Color Vision Genes. Mol Biol Evol. 2004. doi:10.1093/molbev/msh015
20. Kravitz DJ, Saleem KS, Baker CI, Mishkin M. A new neural framework for visuospatial processing. Nature Reviews Neuroscience. 2011. doi:10.1038/nrn3008
21. Hindley EL, Nelson AJD, Aggleton JP, Vann SD. The rat retrosplenial cortex is required when visual cues are used flexibly to determine location. Behav Brain Res. 2014. doi:10.1016/j.bbr.2014.01.028
22. Mao D, Molina LA, Bonin V, McNaughton BL. Vision and Locomotion Combine to Drive Path Integration Sequences in Mouse Retrosplenial Cortex. Curr Biol. 2020. doi:10.1016/j.cub.2020.02.070
23. Fischer LF, Soto-Albors RM, Buck F, Harnett MT. Representation of visual landmarks in retrosplenial cortex. Elife. 2020. doi:10.7554/eLife.51458
24. Alexander AS, Carstensen LC, Hinman JR, Raudies F, William Chapman G, Hasselmo ME. Egocentric boundary vector tuning of the retrosplenial cortex. Sci Adv. 2020. doi:10.1126/sciadv.aaz2322
25. Kothari NB, Wohlgemuth MJ, Moss CF. Dynamic representation of 3D auditory space in the midbrain of the free-flying echolocating bat. Elife. 2018. doi:10.7554/eLife.29053
26. Vann SD, Aggleton JP, Maguire EA. What does the retrosplenial cortex do? Nature Reviews Neuroscience. 2009. pp. 792–802. doi:10.1038/nrn2733 [PubMed: 19812579]
27. Pothuizen HHJ, Davies M, Albasser MM, Aggleton JP, Vann SD. Granular and dysgranular retrosplenial cortices provide qualitatively different contributions to spatial working memory: Evidence from immediate-early gene imaging in rats. Eur J Neurosci. 2009;30: 877–888. doi:10.1111/j.1460-9568.2009.06881.x [PubMed: 19712100]

28. Sugar J, Witter MP, van Strien NM, Cappaert NLM. The Retrosplenial Cortex: Intrinsic Connectivity and Connections with the (Para)Hippocampal Region in the Rat. An Interactive Connectome. Front Neuroinform. 2011 ;5. doi:10.3389/fninf.2011.00007
29. Mao D, Kandler S, McNaughton BL, Bonin V. Sparse orthogonal population representation of spatial context in the retrosplenial cortex. Nat Commun. 2017;8. doi:10.1038/s41467-017-00180-9
30. Mitchell AS, Czajkowski R, Zhang N, Jeffery K, Nelson AID. Retrosplenial cortex and its role in spatial cognition. Brain Neurosci Adv. 2018;2: 239821281875709. doi:10.1177/2398212818757098
31. Vedder LC, Miller AMP, Harrison MB, Smith DM. Retrosplenial Cortical Neurons Encode Navigational Cues, Trajectories and Reward Locations during Goal Directed Navigation. Cereb Cortex. 2017. doi:10.1093/cercor/bhw192
32. Alexander AS, Nitz DA. Spatially Periodic Activation Patterns of Retrosplenial Cortex Encode Route Sub-spaces and Distance Traveled. Curr Biol. 2017. doi:10.1016/j.cub.2017.04.036
33. Alexander AS, Nitz DA. Retrosplenial cortex maps the conjunction of internal and external spaces. Nat Neurosci. 2015; 18: 1143–1151. doi:10.1038/nn.4058 [PubMed: 26147532]
34. Wang Q, Sporns O, Burkhalter A. Network Analysis of Corticocortical Connections Reveals Ventral and Dorsal Processing Streams in Mouse Visual Cortex. J Neurosci. 2012;32: 4386–4399. doi:10.1523/JNEUROSCI.6063-11.2012 [PubMed: 22457489]
35. Waters DA, Vollrath C. Echolocation performance and call structure in the megachiropteran fruit-bat Rousettus aegyptiacus. ACTA CHIROPTEROLOGICA. 2003;5: 209–219.
36. Holland RA, Waters DA, Rayner JMV. Echolocation signal structure in the Megachiropteran bat Rousettus aegyptiacus Geoffrey 1810. J Exp Biol. 2004. doi:10.1242/jeb.01288
37. Zhang W, Yartsev MM. Correlated Neural Activity across the Brains of Socially Interacting Bats. Cell. 2019. doi:10.1016/j.cell.2019.05.023
38. Opalka AN, Huang W qiang, Liu J, Liang H, Wang DV. Hippocampal Ripple Coordinates Retrosplenial Inhibitory Neurons during Slow-Wave Sleep. Cell Rep. 2020. doi:10.1016/j.celrep.2019.12.038
39. Quiroga RQ, Nadasdy Z, Ben-Shaul Y. Unsupervised spike detection and sorting with wavelets and superparamagnetic clustering. Neural Comput. 2004. doi:10.1162/089976604774201631
40. Kobak D, Brendel W, Constantinidis C, Feierstein CE, Kepecs A, Mainen ZF, et al. Demixed principal component analysis of neural population data. Elife. 2016. doi:10.7554/elife.10989
41. Wood ER, Dudchenko PA, Robitsek RJ, Eichenbaum H. Hippocampal neurons encode information about different types of memory episodes occurring in the same location. Neuron. 2000. doi:10.1016/S0896-6273(00)00071-4
42. Beetz MJ, Kordes S, García-Rosales F, Kössl M, Hechavarría JC. Processing of natural echolocation sequences in the inferior colliculus of seba's fruit eating bat, carollia perspicillata. eNeuro. 2017. doi:10.1523/ENEUR0.0314-17.2017
43. Greiter W, Firzlaff U. Representation of three-dimensional space in the auditory cortex of the echolocating bat P. discolor. PLoS One. 2017. doi:10.1371/journal.pone.0182461
44. Measor KR, Leavell BC, Brewton DH, Rumschlag J, Barber JR, Razak KA. Matched behavioral and neural adaptations for low sound level echolocation in a gleaning bat, Antrozous pallidus. eNeuro. 2017. doi:10.1523/ENEURO.0018-17.2017
45. Razak KA, Yarrow S, Brewton D. Mechanisms of sound localization in two functionally distinct regions of the auditory cortex. J Neurosci. 2015. doi:10.1523/JNEUROSCI.2563-15.2015
46. Luo J, Macias S, Ness TV, Einevoll GT, Zhang K, Moss CF. Neural timing of stimulus events with microsecond precision. PLoS Biol. 2018. doi:10.1371/journal.pbio.2006422
47. García-Rosales F, Beetz MJ, Cabral-Calderin Y, Kössl M, Hechavarria JC. Neuronal coding of multiscale temporal features in communication sequences within the bat auditory cortex. Commun Biol. 2018. doi:10.1038/s42003-018-0205-5
48. Yartsev MM, Witter MP, Ulanovsky N. Grid cells without theta oscillations in the entorhinal cortex of bats. Nature. 2011;479: 103–107. doi:10.1038/nature10583 [PubMed: 22051680]
49. Macías S, Luo J, Moss CF. Natural echolocation sequences evoke echo-delay selectivity in the auditory midbrain of the FM bat, eptesicus fuscus. J Neurophysiol. 2018. doi:10.1152/jn.00160.2018

50. Rubin A, Yartsev MM, Ulanovsky N. Encoding of Head Direction by Hippocampal Place Cells in Bats. J Neurosci. 2014;34: 1067–1080. doi:10.1523/jneurosci.5393-12.2014 [PubMed: 24431464]
51. Omer DB, Maimon SR, Las L, Ulanovsky N. Social place-cells in the bat hippocampus. Science (80-). 2018;359: 218–224. doi:10.1126/science.aao3474
52. Brunton BW, Botvinick MM, Brody CD. Rats and Humans Can Optimally Accumulate Evidence for Decision-Making. Science (80-). 2013;340: 95–98. doi:10.1126/science.1233912
53. Erlich JC, Bialek M, Brody CD. A cortical substrate for memory-guided orienting in the rat. Neuron. 2011. doi:10.1016/j.neuron.2011.07.010
54. Heredia-López FJ, Álvarez-Cervera FJ, Collí-Alfaro JG, Bata-García JL, Arankowsky-Sandoval G, Góngora-Alfaro JL. An automated Y-maze based on a reduced instruction set computer (RISC) microcontroller for the assessment of continuous spontaneous alternation in rats. Behav Res Methods. 2016. doi:10.3758/s13428-015-0674-0
55. Zhang Q, Kobayashi Y, Goto H, Itohara S. An automated t-maze based apparatus and protocol for analyzing delay-and effort-based decision making in free moving rodents. J Vis Exp. 2018. doi:10.3791/57895
56. Kugler K, Luksch H, Peremans H, Vanderelst D, Wiegrebe L, Firzlaff U. Optic and echo-acoustic flow interact in bats. J Exp Biol. 2019. doi:10.1242/jeb.195404
57. Horowitz SS, Cheney CA, Simmons JA. Interaction of vestibular, echolocation, and visual modalities guiding flight by the big brown bat, Eptesicus fuscus. J Vestib Res Orientat. 2004;14: 17–32.
58. Rother G, Schmidt U. The Influence of visual Information on echo location in Phyllostomus discolor (Chiroptera). Zeitschrift.fuerSaeugetierkunde. 1982;47: 324–334.
59. Rydell J, Eklöf J. Vision complements echolocation in an aerial-hawking bat. Naturwissenschaften. 2003. doi:10.1007/s00114-003-0464-x
60. Eliav T, Geva-Sagiv M, Finkelstein A, Yartsev MM, Rubin A, Las L, et al. Synchronicity without rhythmicity in the hippocampal formation of behaving bats. Society for Neuroscience Abstract. 2015.
61. Eliav T, Geva-Sagiv M, Yartsev MM, Finkelstein A, Rubin A, Las L, et al. Nonoscillatory Phase Coding and Synchronization in the Bat Hippocampal Formation. Cell. 2018. doi:10.1016/j.cell.2018.09.017
62. Sarel A, Finkelstein A, Las L, Ulanovsky N. Vectorial representation of spatial goals in the hippocampus of bats. Science (80-). 2017;355. doi:10.1126/science.aak9589
63. Geva-Sagiv M, Romani S, Las L, Ulanovsky N. Hippocampal global remapping for different sensory modalities in flying bats. Nat Neurosci. 2016. doi:10.1038/nn.4310
64. Ulanovsky N, Moss CF. Dynamics of hippocampal spatial representation in echolocating bats. Hippocampus. 2011;21: 150–161. [PubMed: 20014379]
65. Yamawaki N, Radulovic J, Shepherd GMG. A Corticocortical Circuit Directly Links Retrosplenial Cortex to M2 in the Mouse. J Neurosci. 2016;36: 9365–9374. doi:10.1523/JNEUROSCI.1099-16.2016 [PubMed: 27605612]
66. Mao D, Neumann AR, Sun J, Bonin V, Mohajerani MH, McNaughton BL. Hippocampus-dependent emergence of spatial sequence coding in retrosplenial cortex. Proc Natl Acad Sci. 2018; 201803224. doi:10.1073/pnas.1803224115
67. Cooper BG, Mizumori SJ. Temporary inactivation of the retrosplenial cortex causes a transient reorganization of spatial coding in the hippocampus. J Neurosci. 2001. doi:21/11/3986 [pii]
68. Smith DM, Barredo J, Mizumori SJY. Complimentary roles of the hippocampus and retrosplenial cortex in behavioral context discrimination. Hippocampus. 2012;22: 1121–1133. doi:10.1002/hipo.20958 [PubMed: 21630374]
69. Aguirre GK, D'Esposito M. Topographical disorientation: a synthesis and taxonomy. Brain. 1999;122: 1613–1628. doi:10.1093/brain/122.9.1613 [PubMed: 10468502]
70. Iaria G, Barton JJS. Developmental topographical disorientation: a newly discovered cognitive disorder. Exp Brain Res. 2010;206: 189–196. doi:10.1007/s00221-010-2256-9 [PubMed: 20431873]

71. Iaria G, Arnold A, Buries F, Liu I, Slone E, Barclay S, et al. Developmental Topographical Disorientation and Decreased Hippocampal Functional Connectivity. Hippocampus. 2014;24: 1364–1374. doi:10.1002/hipo.22317 [PubMed: 24976168]

72. Maguire EA. The retrosplenial contribution to human navigation: A review of lesion and neuroimaging findings. Scand J Psychol. 2001. doi:10.1111/1467-9450.00233

73. Takahashi N, Kawamura M, Shiota J, Kasahata N, Hirayama K. Pure topographic disorientation due to right retrosplenial lesion. Neurology. 1997. doi:10.1212/WNL.49.2.464

Highlights:

- Novel behavioral framework for studying 3D navigation in freely flying bats
- Bats are trained and tested without human interference
- Wireless recordings of behavioral and neural parameters during learning & testing
- Initial application to bat RSC reveals multiplexed coding during aerial navigation

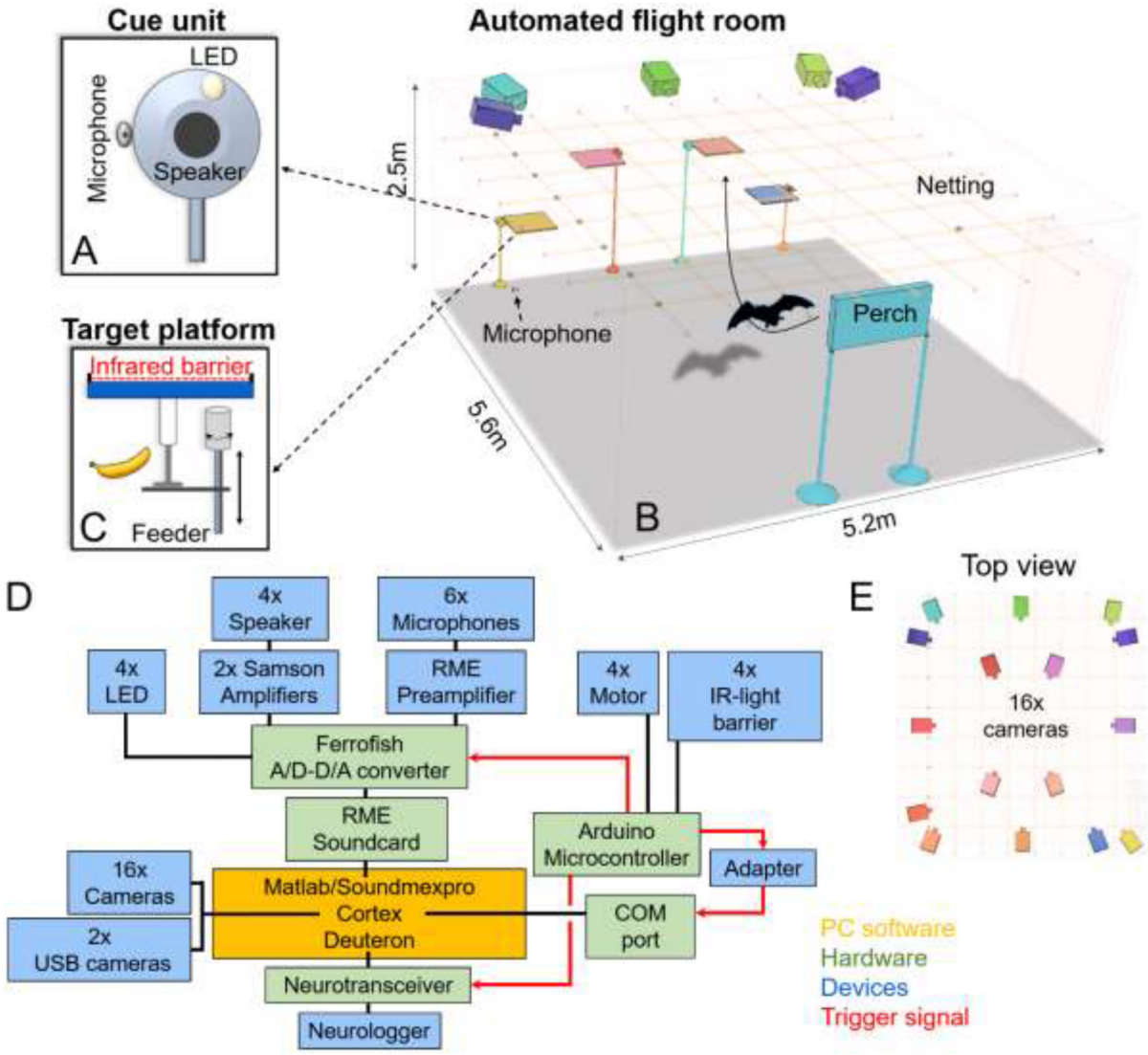

Fig 1: The fully automated bat (FAB) flight room

(A) The present experiment had four cue units (speaker, microphone and small white LED) which are positioned at one end of the room (B), bat image is not-to-scale. The cue unit (A) is positioned next to a landing platform. Each unit is equipped with a reward feeder and an infrared barrier that detects the bats' landing on the platform (C). An additional perch is positioned at the other end of the room. While bats are not constrained in their starting position, all bats self-selected the perch as a starting position for most trials. (D) Schematic of the connectivity diagram of system components, both hardware and software. (E) A 16-camera array mounted on the ceiling monitors the bats' position in 3D space with high spatial and temporal accuracy (only a subset of cameras is depicted in panel B to enhance visibility of the room design).

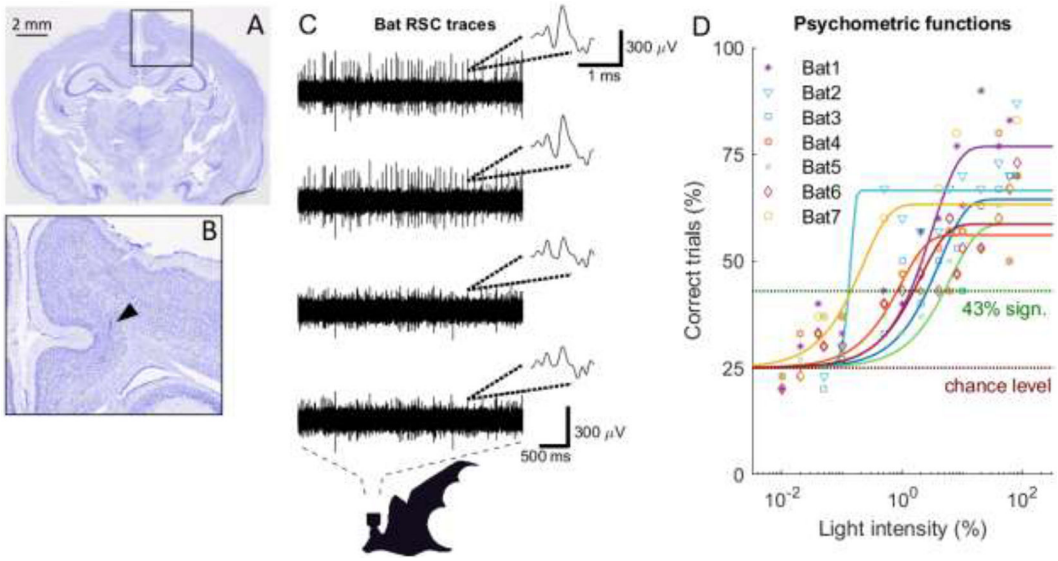

Fig 2: RSC histology verification, RSC neural traces and psychometric functions

(A) Nissl stained coronal section of the bat's brain. (B) Zoom-in on the RSC region where a tetrode track is marked by the black triangle. (C) Example neural traces from the four channels of an example tetrode positioned in the bat RSC. Insets show example waveforms as represented on the four tetrode channels. Time and amplitude scale bars are indicated. (D) Psychometric measurements as a function of light intensity (represented in percentages of the LED being on or off, see Material and Methods) for seven trained bats. Data points for different bats are indicated by different symbols and colors. Fits for each bat are shown (Weibull fit).

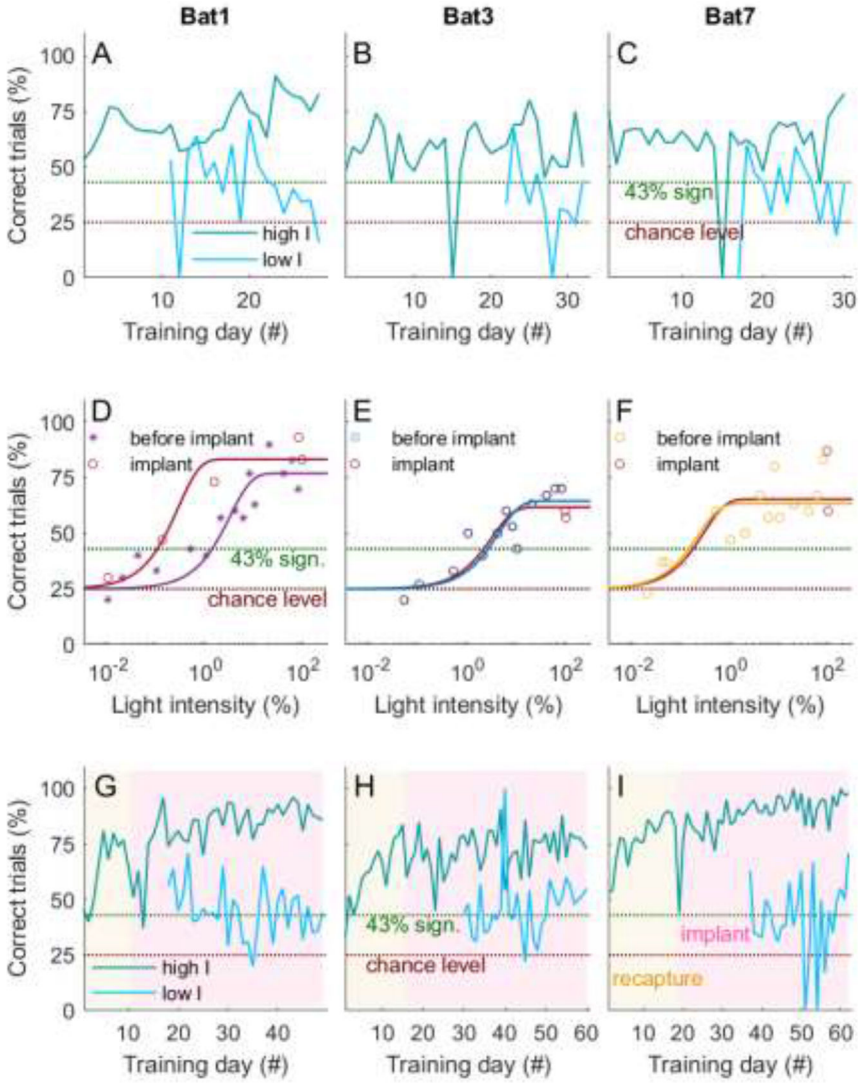

Fig 3: Training consistency and psychometric functions before and after implant

(A-C) Shown are the performance curves (% of correct trials) for the three implanted bats as a function of training day. Trials are separated into high intensities (3% and above, dark cyan) and low intensities (less than 3%, cyan), as this value was slightly above the highest threshold measured for these three bats (2.6% for Bat 3). Chance level is at 25% (4-AFC) and significance at 43% (over 30 trials). During the measurement of the psychometric functions, the bats' performance for the high intensity trials remained stable and above significance level. As expected, the performance for lower intensity levels was lower, between significance and chance, than for the higher intensity trials. The rare performance drops to 0% are due to very low trials numbers (one to a maximum of four trials) as a result of erroneous full-feed of the animals by husbandry care. (D-F) Psychometric functions for light intensities measured before and after implant are highly similar for all three bats, or even shifted towards higher sensitivities (Bat 1). Shown is performance (% of correct trials) as a function of light intensities. Data points are indicated by the symbols and are fitted by a Weibull fit (solid colored lines). (G-I) After recapture of three of the trained bats

(16, six and three months, respectively) the overall performance remained reliably above significance level (indicated by the yellow background). This is also true after the implant of the microdrive (indicated by the red background), especially for the high intensity trials (dark cyan line). Shown are fraction of correct trials against training days. Bat numbers correspond to those introduced in Fig 2.

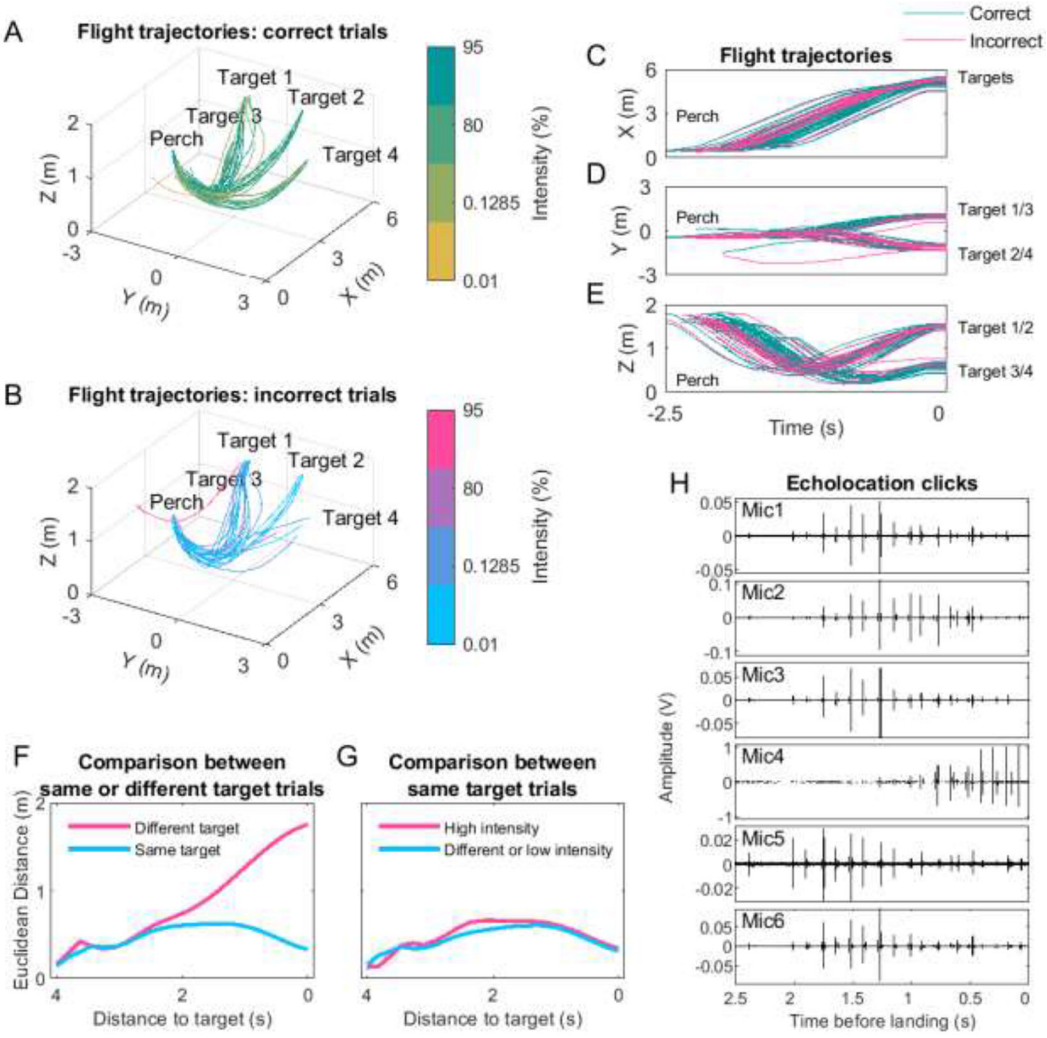

Fig 4: Reproducibility of flight behavior and example echolocation traces

(A-B) Flight trajectories towards the targets for a typical example session. Trials are separated into correct (top) and incorrect (bottom) trials. Light intensity percentage of each trial is color coded (see Material and Methods for values). Note the reproducibility of flight trajectories independent of the approached target, light intensity or reward outcome. The same example session is shown in the panels (C-E), where the trajectories are plotted in time and separated by spatial dimension (X, Y and Z). Correct and incorrect trials are green and magenta, respectively. (F) Comparisons of the 3D Euclidean distances between trials grouped into same or different target (Material and Methods). Shown is the mean and standard error values for each window as a function of distance to the target. The standard errors are very small and therefore barely visible in the plot. Target identity had an effect at a global level and also on trajectory itself (linear mixed model, $p = 0$, LRStat = 5.65×10^5, ΔDF = 1, estimate of fixed effects coefficient (95% CI) of −1415.8 for same or different target and $p = 0$, LRStat = 3.38×10^5, ΔDF = 1, estimate of fixed effects coefficient (95% CI) of 100.8 for the interaction). (G) Same as ‘F’ but comparing same target trials of high intensity (80% and more) with each other or low (less than 80%) with any intensity trials (different; Material and Methods). Light intensity had an effect at a global level and also

on trajectory itself, but this effect was much smaller compared to the target identity effect (linear mixed model, $p = 0$, LRStat = 845.9, ΔDF = 1, estimate of fixed effects coefficient (95% CI) of 33.5 for intensity effect and $p = 0$, LRStat = 1258.1, ΔDF = 1, estimate of fixed effects coefficient (95% CI) of −8.8 for the interaction). Note the small Euclidean distances for the same target trial comparisons indicating a highly stereotyped and reproducible spatial behavior by the bats. (H) Example echolocation traces recorded on the six microphones during the last 2.5 seconds before landing on a platform.

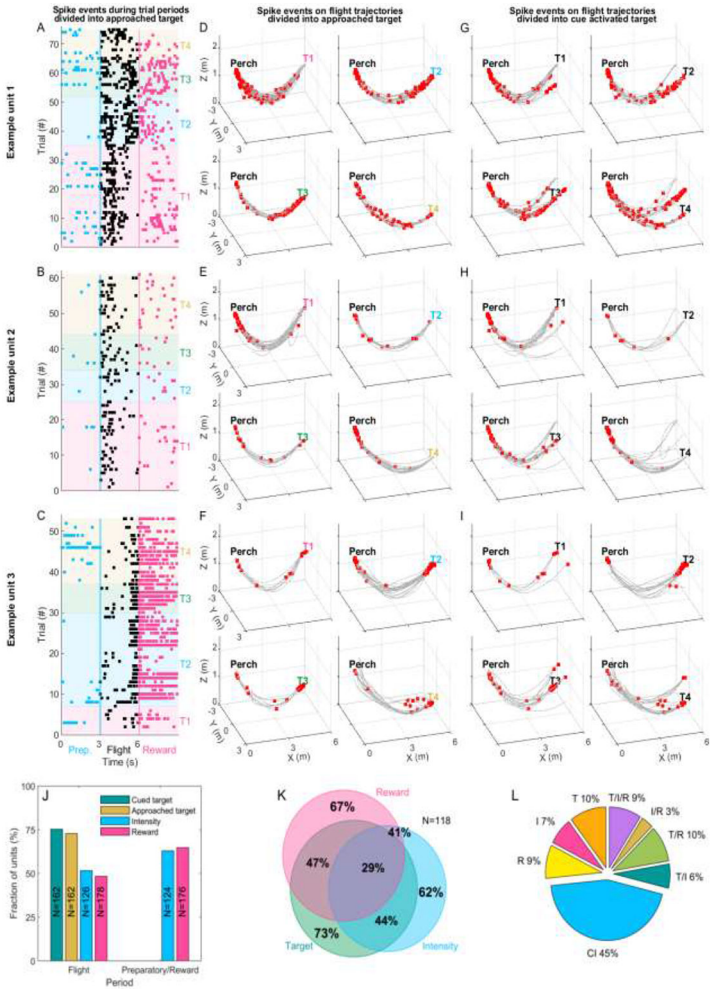

Fig 5: RSC neural activity during the preparatory, flight and reward periods

(A-C) Shown are the spiking events for three example RSC neurons during the preparatory (three seconds before flight), flight and reward (three seconds after landing) periods. The units' spiking events during each trial and the three different periods are color coded (blue=preparatory, black=flight and magenta=reward) and trials are grouped by the targets the bat had approached on a given trial. The approached target is depicted by the colored background (Target 1=magenta, Target 2=blue, Target 3=green and Target 4=ocher). (D-I) Raw 3D spatial spiking activity for the example units. Spikes (red dots) are overlaid on flight trajectories (gray lines). (D-F) Trials are grouped by the approached target and (G-I) trials are group by the cued target. (J) Fraction of significant units for the cued target, approached target, light intensity and the reward outcome (left bars). The two right bars show the fraction of significant units for the preparatory and reward period. The number of units used for calculating significance for a given task variable is indicated for each bar (two-way ANOVA, $p<0.05$). (K) Most neurons were significantly modulated by more than one task variable, shown in the Venn diagram. 'Target' refers to the fraction of units significant for the cued target during flight, 'Intensity' labels the units significant for intensity during the preparatory period and 'Reward' labels the units significant for the bats' decision outcome (or the obtainment of a reward or not) during the reward period. L) Percentages of variance

in the spiking activity explained by the task variables using dPCA. Input components into the dPCA are the task variables (I=Intensity, T=Target and R=Reward) and their interactions (T/I, T/R, I/R and T/I/R). All components independent of the task variables are termed as Condition independent (CI).

Table 1:

Pre-implant behavioral values

The number of psychometric function pre-implant measurement sessions, mean number of trials per session, mean trial times, the overall trial number, psychometric thresholds and the mean flight times for Bats 1-7. Red marked bats correspond to the bats implanted later in the experiment.

Pre-implant	Bat 1	Bat 2	Bat 3	Bat 4	Bat 5	Bat 6	Bat 7
Session (#)	26	28	30	34	34	31	32
Mean trial (#) ± STE	67.5 ± 6.6	41.2 ± 3.7	55.5 ± 6	70.8 ± 5.9	46.9±4.2	59.4 ± 7.2	61.2 ± 6.4
Mean trial time (s) ± STE	6.4 ± 1.1	5.74 ± 2	6.6 ± 1	6.7 ± 1.1	7 ± 0	6.8 ± 0.9	6.4 ± 1.5
Trial (#)	1756	1153	1664	2407	1594	1842	1959
Psychometric threshold (%)	1.4	.1	2.6	.8	5	1.5	.1
Mean flight time (s) ± STD	3 ± 0.6	2.9 ± 1.2	2.9 ± 0.8	2.6 ± 0.6	2.5 ± 0.4	3 ± 0.9	2.8 ± 1

Table 2:

Post-implant behavioral values

The number of psychometric function pre-implant measurement sessions, mean number of trials per session, mean trial times, the overall trial number, psychometric thresholds and the mean flight times for Bats 1, 3 and 7.

Post-implant	**Bat 1**	**Bat 3**	**Bat 7**
Session (#)	49	59	62
Mean trial (#) ± STE	59.7 ± 2	68.3 ± 3.6	48.5 ± 2.4
Mean trial time (s) ± STE	8.8 ± 4.7	7.6 ± 2.5	8.9 ± 2
Trial (#)	2924	4029	3007
Psychometric threshold (%)	.1	.6	.1
Mean flight time (s) ± STD	3.4 ± 1.6	2.8 ± 1.2	2.7 ± 1.4

Table 3:

Pre-implant behavioral performance

The correct performance for each intensity for Bats 1-7 calculated over the last 30 trials, the overall trial number per intensity is indicated in the brackets. Red marked bats correspond to the bats implanted later in the experiment.

Intensity (%)	95	80	60	40	20	10	8	6	4	2	1	.5	.1	.05	.04	.02	.01
Bat 1	80% (292)	70% (130)	83% (126)	77% (149)	90% (154)	63% (159)	77% (131)	57% (119)	60% (105)	57% (94)	40% (65)	43% (38)	33% (30)		40% (30)	30% (60)	20% (98)
Bat 2	63% (278)	87% (148)	70% (132)	73% (118)	67% (94)	70% (67)	57% (57)	67% (38)	57% (30)	57% (30)	60% (30)	67% (30)	30% (30)	23% (30)			
Bat 3	60% (410)	70% (168)	70% (175)	67% (154)	63% (157)	43% (121)	53% (49)	60% (36)	50% (30)	40% (74)	50% (40)	33% (30)	27% (30)	20% (30)			
Bat 4	50% (895)	70% (292)	50% (220)	80% (142)	53% (92)	57% (74)	47% (30)	43% (53)	53% (31)	43% (30)	47% (33)	40% (42)	37% (52)	30% (50)	33% (145)	33% (39)	23% (121)
Bat 5	47% (723)	70% (203)	50% (120)	63% (57)	53% (30)	43% (30)	43% (30)	50% (30)	43% (30)	37% (30)	33% (32)	37% (34)	37% (34)	37% (31)		27% (66)	23% (60)
Bat 6	77% (527)	73% (194)	67% (210)	60% (185)	53% (183)	53% (118)	47% (74)	60% (57)	43% (34)	47% (30)	43% (30)	40% (30)	30% (30)	30% (59)	33% (81)	23% (41)	20% (67)
Bat 7	87% (392)	83% (167)	67% (129)	60% (125)	63% (112)	57% (87)	80% (74)	57% (73)	67% (71)	50% (50)	47% (73)	60% (39)	37% (30)	37% (30)	37% (30)	23% (30)	

Table 4:

Post-implant behavioral performance

The correct performance for each intensity for Bats 1,3 and 7 calculated over the last 30 trials. Overall trial number per intensity is indicated inside the brackets.

Intensity (%)	95	80	1.8864	1.4993	0.1285	.05	.02	.01
Bat 1	83% (1581)	93% (445)		73% (93)	47% (353)			30% (452)
Bat 3	70% (2676)	80% (455)	60% (511)			43% (219)		33% (254)
Bat 7	97% (2531)	93% (178)			57% (162)		33% (69)	37% (67)

Table 5:
Fraction of units significant for the different task variables during flight

Percentage of units significant for the task variables (cued target, approached target, light intensity and reward), the position (divided into three equal parts) and the interaction of each task variable with the position (task variable x position). Two-way ANOVA, $p<0.5$.

Task variable	Significant for task variable	Significant for position	Significant for interaction (task variable x position)
Cued target	75.3%	93.2%	71%
Approached target	72.8%	92.6%	84.4%
Light intensity	51.6%	92.1%	48.4%
Reward	48.3%	89.9%	55.1%